Controlled FRET efficiency in nano–bio hybrid materials made from semiconductor quantum dots and bacteriorhodopsin

Nicolas Bouchonville[a], Anthony Le Cigne[a], Alyona Sukhanova[b,c], Marie-belle Saab[a], Michel Troyon[a], Michael Molinari[a], Igor Nabiev*[b,c]

[a]Laboratory of Research in Nanotechnology, University of Reims Champagne-Ardenne, 21 rue Clément Ader, 51685 Reims Cedex 2, France; [b]Laboratory of Nano-Bioengineering, Moscow Engineering Physics Institute, 31 Kashirskoe sh., 115409 Moscow, Russian Federation; [c]European Technological Platform "Semiconductor Nanocrystals," Institute of Molecular Medicine, James's Street, Trinity College Dublin, Dublin 8, Ireland

ABSTRACT

Förster resonance energy transfer (FRET) between CdSe/ZnS core/shell quantum dots (QDs) and the photochromic protein bacteriorhodopsin (bR) in its natural purple membrane (PM) has been modulated by independent tuning of the Förster radius, overlap integral of the donor emission spectrum and acceptor absorption spectrum, and the distance between the donor (QD) and acceptor (bR retinal). The results have shown that the observed energy transfer from QDs to bR corresponds to that predicted by a multiple-acceptors geometric model describing the FRET phenomenon for QDs quasi-epitaxied on a crystalline lattice of bR trimers. Linking of QDs and bR via streptavidin–biotin linkers of different lengths caused FRET with an efficiency reaching 82%, strongly exceeding the values predicted by the classical FRET theory. The data not only demonstrate the possibility of nano-bioengineering of efficient hybrid materials with controlled energy-transfer properties, but also emphasize the necessity to develop an advanced theory of nano–bio energy transfer that would explain experimental effects contradicting the existing theoretical models.

Keywords: bacteriorhodopsin, quantum dots, hybrid materials, FRET, photovoltaics, nano-biotechnology, biophotonics

1. INTRODUCTION

Light-harvesting nano–bio hybrid materials play an increasingly important role as an alternative to devices utilizing lithographic techniques, and they may occupy a niche in nano-biophotonics and biophotovoltaics. Protein-based photonic devices have been paid special attention because of the possibility to control the functional and optical properties of proteins through chemical modifications, genetic engineering, and specific spatial organization via self-assembly[1]. Although various proteins have been used in designing such devices[2-4], the membrane protein bacteriorhodopsin (bR) has attracted most attention[5]. bR is a single integral protein of purple membranes (PMs) of *Halobacterium salinarum*, in which it forms trimers arranged in a regular two-dimensional crystalline network with a lattice constant of 6.2 nm[6]. Absorption of light by the single protein-linked chromophore (retinal) lead to photoisomerization of the retinal and cyclic sequence of spectrally distinguishable protein conformational transitions resulting in transport of protons from the cytoplasm to the outer side of the cell membrane. This proton transport creates an electrochemical gradient, which drives ATP synthesis[7]. bR has evolved as a protein extremely resistant to thermal, chemical, and photochemical degradation, which makes it one of the most promising candidates for development of protein-based devices[1,5]. As such, it has been used for development of photoreceivers[8], transceivers[9], optical switches[10], molecular engines[11], and electronic switches[12] and was also used for light-driven production of ATP[13].

* igor.nabiev@gmail.com

Biosensing and Nanomedicine V, edited by Hooman Mohseni, Massoud H. Agahi, Manijeh Razeghi,
Proc. of SPIE Vol. 8460, 84600X · © 2012 SPIE · CCC code: 0277-786/12/$18 · doi: 10.1117/12.930747

Although bR fulfils perfectly its biological function, it should be re-engineered to meet the requirements for industrial hybrid materials used in competitive photonic and photovoltaic applications. One of common limitations of photosensitive proteins in such applications is their inability to collect light in a broad range of wavelengths, especially the inability to absorb high-energy photons of the UV region of the optical spectrum, which may damage the absorbing chromophores[14].

Semiconductor quantum dots (QDs) are inorganic nanoparticles that can very efficiently absorb photons in the UV and visible regions of the optical spectrum and convert their energy into that of a narrow photoluminescence (PL) emission in the spectral region varying as a function of the QD size[15,16,17]. Recently, we have used CdSe/ZnS and CdTe QDs as light-harvesting collectors and transceivers of the solar energy in the UV to blue region of the optical spectrum transferring it to specialized light-harvesting chromophores of photosynthetic reaction centers (RCs)[18] and bR in its natural PMs[19]. The nano–bio hybrid systems have been carefully engineered in such a way that QDs (energy donors) transfer the collected energy to the chromophores of photosensitive proteins (acceptors) via Förster resonance energy transfer (FRET) with an efficiency approaching 100%, thus improving the biological functions of the acceptors. The structure of the complexes made of CdSe/ZnS QDs and bR-containing PMs have been further investigated by means of atomic force microscopy (AFM) imaging, which has demonstrated that the most FRET-efficient QD–PM complexes are characterized by the highest level of QD orderliness correlating with that of the bR-trimer arrangement within the PM[20].

In this study, we have shown that the efficiency of FRET within a bR–QD hybrid material may be carefully controlled by varying the Förster radius and tuning the PM thickness and the spectral overlap of the QD emission and bR absorption spectra. In these cases, the observed experimental parameters correspond to those predicted by the classical FRET theory based on a geometrical multiple-acceptors model of QD–PM complexes deduced from our previous AFM imaging data[19,20]. In contrast, QD–bR linking using streptavidin–biotin linkers of different lengths caused FRET with an efficiency reaching 82%, strongly exceeding the values predicting by the classical FRET theory. These experimental data indicate the necessity of new theoretical approaches to the analysis of FRET in nano–bio hybrid materials on the nanoscale in order to explain the experimental effects contradicting the classical theoretical models.

2. THEORY

2.1. The theoretical multi-acceptors FRET model

FRET is nonradiative energy transfer between donor chromophores in an excited state (D) and acceptor chromophores in their ground state (A)[21]. One of the key parameters determining the efficiency of FRET is the Förster radius ($\boldsymbol{R_0}$) defined as the distance between D and A for which the FRET efficiency approaches 50%. It can be calculated from the intrinsic optical and spectral parameters of D and A:

$$R_0^6 = \frac{9000(\ln 10)Q_D\kappa^2}{128\pi^5 N n^4} J(\lambda) \qquad \text{(Eq. 1)}$$

where $\boldsymbol{Q_D}$ is the donor quantum yield, $\boldsymbol{\kappa^2}$ is the transition dipole orientation factor, $\boldsymbol{N}$ is Avogadro's number, $\boldsymbol{n}$ is the refractive index of the medium and $\boldsymbol{J(\lambda)}$ is the normalized overlap integral between the D emission and A absorption.

The normalized overlap integral is calculated as follow:

$$J(\lambda) = \int_0^\infty F_D(\lambda)\varepsilon_A(\lambda)\lambda^4 d\lambda \qquad \text{(Eq. 2)}$$

where $\boldsymbol{F_D}$ is the normalized emission of $\boldsymbol{D}$, and $\boldsymbol{\varepsilon_A}$ is the molar absorption coefficient of A at the wavelength $\boldsymbol{\lambda}$.

The FRET efficiency ($\boldsymbol{E}$), which reflects the theoretical fraction of absorbed photons transferred to the acceptor at a given distance, can be determined using the following equation:

$$E = \frac{n_A R_0^6}{n_A R_0^6 + r^6} \qquad \text{(Eq. 3)}$$

where R_0 is the Förster radius, r is the distance between the donor and the acceptor (the D–A distance), and n_A is the number of acceptors accessible for energy transfer from the donor. Note that the above equations pertain to the "classical" FRET theory assuming the presence of an exciton with an asymmetric wave function around the nanocrystal center, which may not be always the case[22,23].

In the case of nano-hybrid materials that we have engineered from QDs and bR, previous AFM results fit a multiple-acceptors geometric model describing FRET between QDs quasi-epitaxied on a crystalline lattice made of bR trimers where the energy harvested by QDs may be efficiently transferred to the three retinal chromophores of a bR trimer[20]. This model has been subsequently used to calculate theoretical donor–acceptor distances and theoretical FRET efficiencies in order to provide a basis for comparison of the experimental and "classical" theoretical FRET efficiency values.

2.2. The geometrical model for calculation of the theoretical donor–acceptor distance (r_{th})

A geometrical model was elaborated in order to compare the D–A distance calculated in terms of the multi-acceptors FRET theory and FRET efficiencies measured in steady-state experiments with the shortest possible D–A distances. In this model, we assume that there is one bound QD per bR trimer (according to the AFM imaging data) and that this QD is at equal distances from all three retinals of this trimer. Additionally, we assume that all r_{th} values are measured between the retinal and the center of the QD. The classical Förster theory treats the donors and the acceptors as point dipoles in the interaction space, although QDs have a finite size and are relatively large compared to the retinal[24].

Since bRs are organized in trimers within the PMs, retinals are also organized in this way and located close to the middle of the PM, about 2.5 nm from each surface. Since the PM thickness is dependent on its environment (pH, ionic strength of the buffer solution, and humidity)[25], we have also included PM thickness (e) as a parameter of our model.

Figure 1 shows the geometry of the QD–PM system and demonstrates that r_{th} can be calculated as follows:

$$r_{th} = \sqrt{d^2 + (e/2 + R)^2} \qquad \text{(Eq. 4)}$$

where d is the distance from the retinal to the center of the triangle formed by the bR molecules, e is the thickness of the PM, and R is the total radius of the QD (core + shell + organic ligands). Since the distance between two bRs is 3.5 nm (Figure 1), d is assumed to be 2 nm.

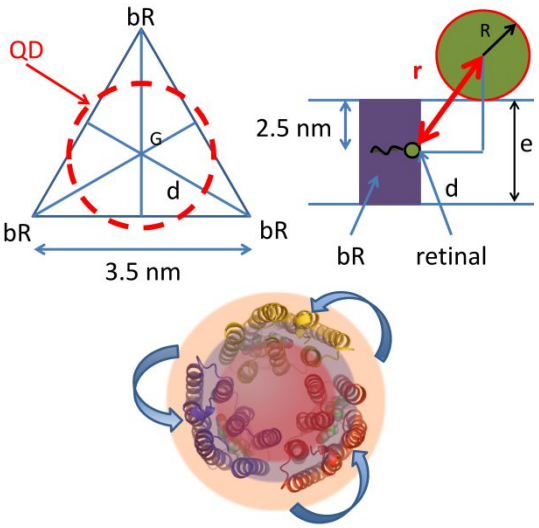

Figure 1. The multiple-acceptors FRET geometrical model based on the structural results of Refs. 20, 21 and illustrating the result of the use of Eq. 4 to calculate the theoretical donor–acceptor distances in the bR–QD nano–bio hybrid material.

A QD is located on a bR trimer and can efficiently transfer the harvested energy to three bR retinals located approximately in the center of the purple membrane.

The thickness of the PM (e) is assumed to be 5 nm, but it may slightly vary depending on the external conditions (including pH and ionic strength).

3. MATERIALS AND METHODS

Purple membranes containing wild-type bR were prepared and purified according to the protocol adapted from Ref. 26. The PMs were dissolved in buffer solutions with a desired pH to obtain a stock solution with an optical density of about 0.2 at 568 nm.

CdSe/ZnS core/shell QDs were synthesized as described in Refs. 26, 27. Postsynthetic TOPO ligands were replaced from the QD surface using DL-Cys or three-functional polyethylenglycols, as described earlier[28,29]. QDs were then dissolved in different buffer solutions, depending on their new ligands. Cystein-coated and PEG-COOH-coated QDs were dissolved in a TRIS buffer solution at pH 8.8, cysteamine-coated QDs were dissolved in MES at pH 5.0, and PEG-OH-coated QDs were stable at pH values of 8.8, 7.0, or 5.0. The hydrodynamic diameters and zeta-potentials of QDs were measured with a Malvern Nano ZS device. Cystein- and cysteamine-coated QDs were found to have a hydrodynamic diameter of 7 nm; the diameter of PEGylated QDs was about 9 nm. Cysteine-coated and PEG-COOH-coated QDs have a zeta-potential of about –35 mV, PEG-OH-coated QDs have a zeta-potential of –5 mV, and cysteamine-coated QDs have a zeta-potential of about +30 mV.

For bR–QD biotin–streptavidin linking, QDs were conjugated with streptavidin according to the protein-binding protocol described earlier[28,29]; the amino groups of bR within PMs were biotynilated with NHS-biotin, NHS-LC-biotin, or NHS-LC-LC-biotin using a commercial kit purchased from Thermoscientific as recommended by the supplier[30].

4. RESULTS

4.1 Effect of variation of the overlap integral (*J*) on the FRET efficiency in the QD–bR hybrid system

As follows from Eq. 1, the FRET efficiency should depend on the overlap between the D fluorescence and A absorption spectra. This dependence is quantified by the overlap integral $\boldsymbol{J}$, which can be calculated only from the D and A optical parameters (Eq. 2) and strongly affects the Förster radius. Since QD properties are size-dependent, the spectral overlap of QD emission with bR absorption can be modified by tuning the QD size. Aqueous solutions of QDs with emission wavelengths of 570, 610, and 650 nm were prepared and solubilized with DL-Cys (Figure 2). Since the bR absorption maximum is at 568 nm, the QDs of the three fluorescence colors exhibited the maximum, partial, and minimum spectral overlaps with the bR absorption, respectively (Figure 2). This is clearly demonstrated by the more than twofold difference between the calculated $\boldsymbol{J}$ values for the QDs with the best overlap with the bR absorption spectrum and QDs with the worst one: 6.32×10^{15} for the QDs emitting at 570 nm versus 2.79×10^{15} for the QDs emitting at 650 nm (Table 1). This difference in the overlap integrals $\boldsymbol{J}$ determines a variation of the Förster radius $\boldsymbol{R_0}$ of more than 1 nm (Eq. 2). It is worth mentioning that even so small a variation of the Förster radius results in a considerable variation of the FRET efficiency due to the factor $\boldsymbol{R_0^6}$ in the equation determining the FRET efficiency $\boldsymbol{E}$ (Eq. 3).

Table 1. Comparison of the theoretical and experimental parameters of energy transfer within three bR–QD hybrid materials engineered by self-assembly of purple membranes with the QDs (Figure 1) of three different colors (diameters) solubilized with DL-Cys, which have different values of the overlap integral (Figure 2).

Sample / parameter	$\boldsymbol{J}$ (M^{-1} cm^{-1} nm^4) Overlap integral	$\boldsymbol{R_0}$ (nm) Förster radius	$\boldsymbol{r_{th}}$ (nm) Theor. r_{DA} distance	$\boldsymbol{r_{exp}}$ (nm) Exper. r_{DA} distance	$\boldsymbol{E_{th}}$ (%) Theor. FRET efficiency	$\boldsymbol{E_{exp}}$ (%) Exper. FRET efficiency
PM–QD570	6.32E+15	4.96	5.70	5.53	56	61
PM–QD610	5.05E+15	4.60	6.26	6.76	32	23
PM–QD650	2.79E+15	3.85	7.08	6.80	7.2	9

Our experimental data on the steady-state fluorescence measurements of QD in solutions with different bR concentrations (Figure 2) showed that the FRET efficiency was the highest (61%) for QDs emitting at 570 nm (QD570), which were also characterized by the highest ***J*** (Table 1). QD610 and QD650 exhibited FRET efficiencies of 23% and 9%, respectively (Figure 2B). Since the QD fluorescence red-shifted with increasing QD diameter, the distance between the bR retinal and the QD center for which the FRET donor–acceptor distance was measured was also increased. These parameters were taken into account for precise comparison of the FRET theory prediction with the experimental data. The data of Table 1 show that the differences between the theoretical and experimental values did not exceed 10%, thus indicating good agreement between the classical FRET multiple-acceptors theoretical model and experimental data.

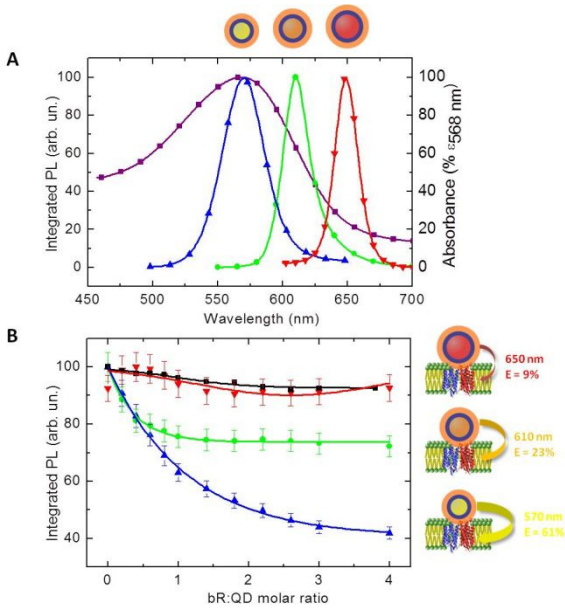

Figure 2. Experimental effect of variation of the overlap integral between QD fluorescence emission and bR absorption on the efficiency of energy transfer within self-assembled bR–QD hybrid materials.

Panel A: QDs of three different fluorescence colors (570, 610, and 650 nm) were synthesized and solubilized with DL-Cys in exactly the same manner. These three batches of QDs exhibited distinctly different overlaps between their fluorescence emissions (the blue, green, and red curves, respectively) and bR absorption (the violet curve).

Panel B: Steady-state quenching of the fluorescence of QDs of different colors shown in Panel A upon their self-assembling with PMs at different bR to QD molar ratios.

The blue, green, and red curves correspond to quenching of the QDs emitting fluorescence at 570, 610, and 650 nm, respectively. The black curve corresponds to the control experiment on the quenching of QDs with "white membranes" (PMs from which retinal was carefully extracted). White membranes are an excellent negative control for FRET experiments because the acceptor (retinal) is absent, so that QD fluorescence quenching with white membranes may be caused only by mechanisms not related to FRET.

4.2 Variation of the donor–acceptor distance by varying the thickness of the purple membrane

Since FRET is highly sensitive to the donor–acceptor distance (Eq. 3), even small variation of this distance should strongly affect the FRET-efficiency. It is also known that the thickness of the lipid bilayer is highly sensitive to pH. Since PMs are mainly composed of lipids, their thickness is also strongly pH-dependent.[25] We have used this fact to vary the distance between QDs and the retinals of bRs (located in the middle of the membrane) and to analyze if the experimentally measured variation of the FRET efficiency fit the values predicted by the classical multiple-acceptors FRET theory (Eqs. 1–4).

Table 2. Comparison of the theoretical and experimental parameters of energy transfer upon pH-controlled variations of the thicknesses of the purple membrane (Figure 3) causing small changes in the donor–acceptor distances in the bR–QD hybrid material.

Sample / Parameter	**pH**	**Membrane thickness (nm)**[30]	R_0 (nm) Förster radius	r_{th} (nm) Theor. r_{DA} distance	r_{exp} (nm) Experim. r_{DA} distance	E_{th} (%) Theor. FRET efficiency	E_{exp} (%) Experim. FRET efficiency
PM–(QD–PEGOH) $\lambda_{em.}$ = 570 nm	**7.0**	**5.7**	5.52	9.40	9.39	10.9	11
	8.8	**5.5**	5.52	9.31	8.97	11.5	14
	5.0	**5.25**	5.52	9.18	8.44	12.4	19

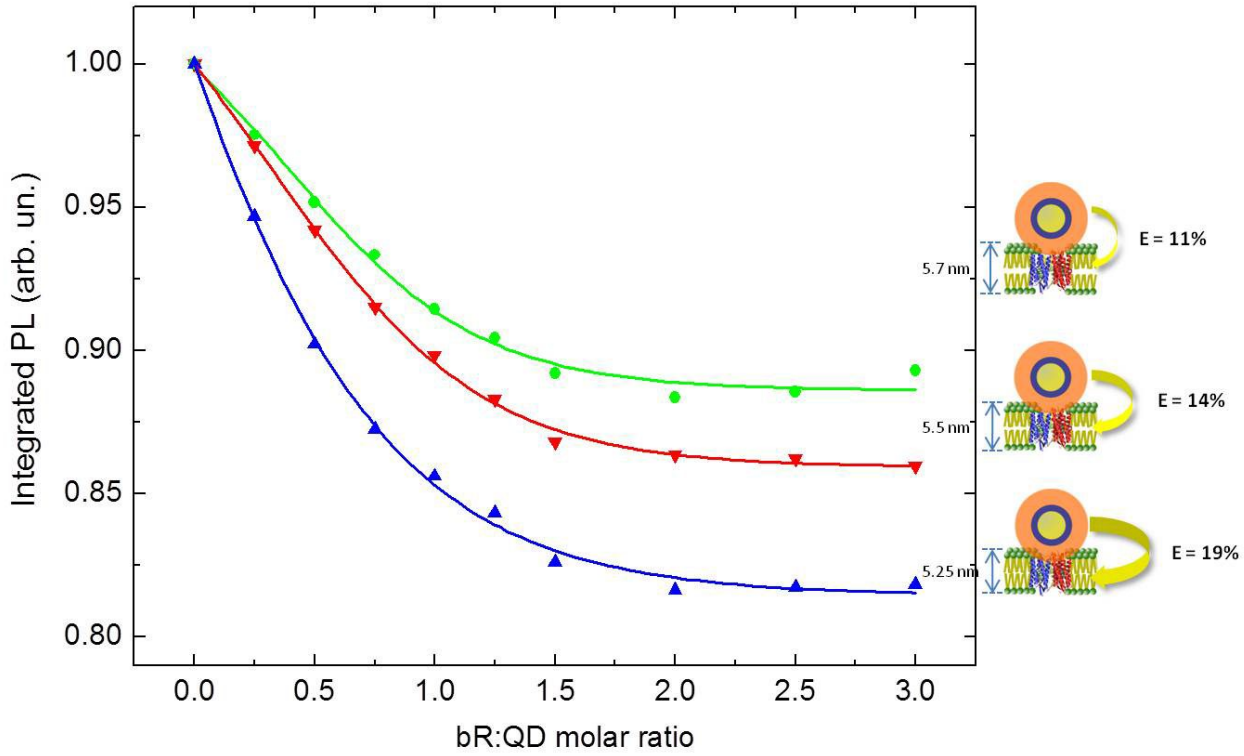

Figure 3. Experimental effects of pH-controlled variation of the thickness of the purple membrane (PM) on the efficiency of energy transfer from QDs to bR within self-assembled bR–QD hybrid materials.

The blue, red, and green curves correspond to the steady-state fluorescence analysis of QD fluorescence quenching upon their self-assembling with the PMs at pH values of 5, 8.8, and 7.0, respectively. Variation of pH induces variation of the thickness of the PM, which was monitored by AFM measurements as described earlier[30]. The data shows that the efficiency of energy transfer directly correlates with the variation of the donor–acceptor distance caused by changes in the PM thickness (Table 2).

The PEG-OH-covered QDs emitting fluorescence at 570 nm were dispersed in buffer solutions with different pH values. The PM thickness is known to vary at different pH values, thus changing the donor–acceptor distance from 9.18 to 9.40 nm (Table 2). As predicted by the FRET theory, the experimentally measured energy transfer efficiencies were found to be dependent on the PM thickness (Figure 3). Comparison of the data show that the experimentally measured FRET efficiencies are in excellent agreement with the data calculated on the basis of the classical FRET theory (Table 2).

4.3 Engineering of a QD–bR hybrid material with the use of streptavidin–biotin linkers of different lengths.

Biotin–streptavidin linking is known to be the strongest biological linking with a dissociation constant comparable with that of covalent binding (from 10^{-14} to 10^{-16} M)[31]. Since bR can be biotinylated[30] and QDs can be covered with streptavidin[26,27], this specific and strong interaction may be used to link bR to QDs in a controlled way. Moreover, the bR–QD distance in this complex may be additionally varied using modified biotins containing additional "long chain" linkers about 13 Å in length.

We biotinylated PMs using NHS-biotin, NHS-LC-biotin, and NHS-LC-LC-biotin and analyzed the efficiency of the energy transfer from streptavidinated QDs to biotinylated PMs using steady-state fluorescence measurements for these systems (Figure 4). The data show that the maximum FRET efficiency of 82% was achieved with the use of the shortest biotin linker and efficiencies of 63% and 50%, in the cases of biotin-LC and biotin-LC-LC linkers, respectively.

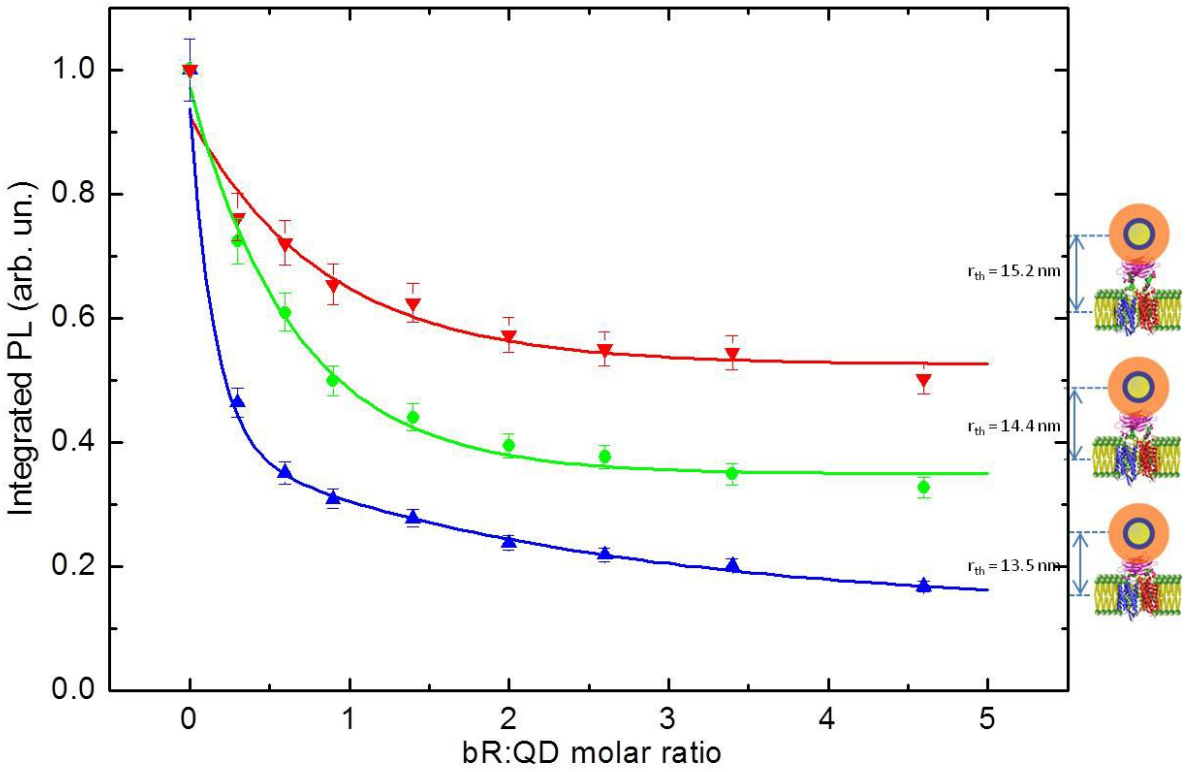

Figure 4. The efficiencies of energy transfer within QD–bR hybrid materials engineered through biotin–streptavidin linkage of streptavidinated QDs to PMs biotinylated using modified biotin linkers of different lengths.

Theoretical calculations according to the classical FRET theory should, which took into account the diameter of the streptavidine molecule in its globular form (5 nm) and lengths of different biotin linkers, yielded the values of FRET efficiencies (1.28%, 0.87% and 0.63%, respectively) that were much smaller than our experimental values. This dramatic difference between the experimental and theoretical values clearly indicates the necessity of understanding of the structural phenomena on the interface between the nano- and bio-components of the hybrid materials developed (Table 3).

Table 3. Comparison of the theoretical and experimental parameters of energy transfer in the systems engineered through biotin–streptavidine coupling of streptavidinated QDs and PMs biotinilated with biotin linkers of different lengths (Figure 4).

Sample/Parameter		R_0 **(nm)** Förster radius	r_{th} **(nm)** Theor. r_{DA} distance	r_{exp} **(nm)** Experim. r_{DA} distance	E_{th} **(%)** Theor. FRET efficiency	E_{exp} **(%)** Exper. FRET efficiency
(PM-biotin)-(QD-streptavidine) $\lambda_{em.}$ = 570 nm	**biotin-LC-LC**	5.45	15.2	6.55	0.63	50
	biotin-LC	5.45	14.4	5.99	0.87	63
	biotin	5.45	13.5	5.08	1.28	82

5. CONCLUSION

We have demonstrated the possibility of precise control of the FRET efficiency within QD–bR hybrid systems through fine tuning of the overlap integral between the QD fluorescence emission and bR absorption spectra and the distance between the donor (QD) and acceptor (bR retinal located at the centre of the purple membrane). Electrostatic self-assembling of QDs and PMs or (QD–streptavidine)–(PM–biotin) linking were used to achieve FRET efficiencies exceeding 80%. Comparison of experimental data and theoretical calculations based on the classical multiple-acceptors model has demonstrated excellent agreement between the theoretical predictions and the results of experiments on tuning the overlap integral with the use of QD of different colors and on varying the thickness of the PM using external environmental factors.

On the other hand, coupling of QDs and bR using a streptavidin–biotin complex with linkers of different lengths caused FRET with efficiencies strongly exceeding the values predicted by the classical FRET theory. This dramatic difference between the experimental and theoretical values clearly indicates the necessity of understanding structural phenomena at the interface between the nano- and bio-components of the hybrid materials developed. The data not only demonstrate the possibility of nano-bioengineering of efficient hybrid materials with controlled energy transfer properties, but also emphasize the necessity to develop an advanced theory of nano–bio energy transfer that would explain the experimental effects contradicting the existing theoretical models. The last but not least important result is that the effects occurring at the interface of nanoparticles and biological molecules may strongly influence the biomolecule function, thus creating potential hazards that should be predicted in advance and attentively controlled if safely nano–bio hybrid devices are to be constructed.

6. ACKNOWLEDGMENTS

This study was supported by the Ministry of Education and Science of the Russian Federation (grant no. 11.G34.31.0050) and the European Commission through the FP7 Cooperation Program (grant no. NMP-2009-4.0-3-246479 NAMDIATREAM). We thank Vladimir Ushakov for the help in the preparation of the manuscript.

REFERENCES

[1] Birge, R. R., Gillespie, N. B., Izaguirre, E. W., Kusnetzow, A., Lawrence, A. F., Singh, D., Song, Q. W., Schmidt, E., Stuart, J. A., Seetharaman, S. and Wise, K. J., "Biomolecular Electronics: Protein-Based Associative Processors and Volumetric Memories," J. Phys. Chem. B, 103(49), 10746-10766 (1999).

[2] Hampp, N. and Oesterhelt, D., [Bacteriorhodopsin and Its Potential in Technical Applications] Wiley-VCH Verlag GmbH & Co. KGaA, Berlin(2005).

[3] Lee, I., Lee, J. W. and Greenbaum, E., "Biomolecular Electronics: Vectorial Arrays of Photosynthetic Reaction Centers," Phys. Rev. Lett., 79(17), 3294-3297 (1997).

[4] Vsevolodov, N. N., [Biomolecular electronics: an introduction via photosensitive proteins] Birkhauser, Boston-Basel-Berlin (1998).

[5] Hampp, N., "Bacteriorhodopsin as a photochromic retinal protein for optical memories," Chem. Rev. 100(5), 1755-1776 (2000).

[6] Butt, H. J., Downing, K. H., and Hansma, P. K., "Imaging the membrane protein bacteriorhodopsin with the atomic force microscope," Biophys. J. 58(6), 1473-80 (1990).

[7] Oesterhelt, D. and Stoeckenius, W., "Isolation of the cell membrane of Halobacterium halobium and its fractionation into red and purple membrane," Meth. Enzymol. 31, 667-678 (1974).

[8] Shin, J., Bhattacharya, P., Yuan, H. C., Ma, Z. and Varo, G., "Low-power bacteriorhodopsin-silicon n-channel metal-oxide field-effect transistor photoreceiver," Opt. Lett. 32(5), 500-2 (2007).

[9] Shin, J., Bhattacharya, P., Xu, J. and Varo, G., "Monolithically integrated bacteriorhodopsin-GaAs/GaAlAs phototransceiver," Opt. Lett. 29(19), 2264-6 (2004).

[10] Dér, A., Valkai, S., Fábián, L., Ormos, P., Ramsden, J. J. and Wolff, E. K., "Integrated optical switching based on the protein bacteriorhodopsin," Photochem. Photobiol. 83(2), 393-396 (2007).

[11] Samoilovich, M. I., Belyanin, A. F., Grebennikov, E. P. and Guriyanov, A. V., "Bacteriorhodopsin—the basis of molecular superfast nanoelectronics," Nanotechnol. 13(6), 763-767 (2002).

[12] Pandey, P., "Bacteriorhodopsin—Novel biomolecule for nano devices," Anal. Chim. Acta 568(1-2), 47-56 (2006).

[13] Wendell, D. W., Patti, J. and Montemagno, C. D., "Using biological inspiration to engineer functional nanostructured materials," Small 2(11), 1324-1329 (2006).

[14] Lao, K. and Glazer, A. N., "Ultraviolet-B photodestruction of a light-harvesting complex," Proc. Natl. Acad. Sci. USA 93(11), 5258-5263 (1996).

[15] Chan, W. C., Maxwell, D. J., Gao, X., Bailey, R. E., Han, M. and Nie, S., "Luminescent quantum dots for multiplexed biological detection and imaging," Curr. Opin. Biotechnol. 13(1), 40-46 (2002).

[16] Resch-Genger, U., Grabolle, M., Cavaliere-Jaricot, S., Nitschke, R. and Nann, T., "Quantum dots versus organic dyes as fluorescent labels," Nature Meth. 5(9), 763-775 (2008).

[17] Sukhanova, A. and Nabiev, I., "Fluorescent nanocrystal quantum dots as medical diagnostic tools," Expert Opin. Med. Diagn. 2(4), 429-447 (2008).

[18] Nabiev, I., Rakovich, A., Sukhanova, A., Lukashev, E., Zagidullin, V., Pachenko, V., Rakovich, Y. P., Donegan, J. F., Rubin, A. B. and Govorov, A. O., "Fluorescent quantum dots as artificial antennas for enhanced light harvesting and energy transfer to photosynthetic reaction centers," Angew. Chem. Intl. Ed. 49(40), 7217-7221 (2010).

[19] Rakovich, A., Sukhanova, A., Bouchonville, N., Lukashev, E., Oleinikov, V., Artemyev, M., Lesnyak, V., Gaponik, N., Molinari, M., Troyon, M., Rakovich, Y. P., Donegan, J. F. and Nabiev, I., "Resonance energy transfer improves the biological function of bacteriorhodopsin within a hybrid material built from purple membranes and semiconductor quantum dots," Nano Lett. 10(7), 2640-2648 (2010).

[20] Bouchonville, N., Molinari, M., Sukhanova, A., Artemyev, M., Oleinikov, V. A., Troyon, M. and Nabiev, I., "Charge-controlled assembling of bacteriorhodopsin and semiconductor quantum dots for fluorescence resonance energy transfer-based nanophotonic applications," Appl. Phys. Lett. 98(1), 013703 (2011).

[21] Lakowicz, J. R., [principles of fluorescence spectroscopy] Springer, New York (2006).

[22] Efros, A. L. and Rosen, M., "The electronic structure of semiconductor nanocrystals," Annu. Rev. Mater. Sci. 30, 475-521 (2000).

[23] Gaponenko, S. V., [Optical properties of semiconductor nanocrystals], Cambridge University Press, Cambridge (1998).

[24] Wargnier, R., Baranov, A. V., Maslov, V. G., Stsiapura, V., Artemyev, M., Pluot, M., Sukhanova, A. and Nabiev, I., "Energy transfer in aqueous solutions of oppositely charged CdSe/ZnS core/shell quantum dots and in quantum dot−nanogold assemblies," Nano Lett. 4(3), 451-457 (2004).

[25] Müller, D., Schabert, F. A., Büldt, G., and Engel, A., "Imaging purple membranes in aqueous solutions at sub-nanometer resolution by atomic force microscopy," Biophys. J., 68(5), 1681-1686 (1995).

[26] Sukhanova, A., Devy, J., Venteo, L., Kaplan, H., Artemyev, M., Oleinikov, V., Klinov, D., Pluot, M., Cohen, J. H. M. and Nabiev, I., "Biocompatible fluorescent nanocrystals for immunolabeling of membrane proteins and cells," Anal. Biochem. 324(1), 60-67 (2004).

[27] Sukhanova, A., Venteo, L., Devy, J., Artemyev, M., Oleinikov, V., Pluot, M. and Nabiev, I., "Highly stable fluorescent nanocrystals as a novel class of labels for immunohistochemical analysis of paraffin-embedded tissue sections," Lab. Invest. 82(9), 1259-1261 (2002).

[28] Nabiev, I., Mitchell, S., Davies, A., Williams, Y., Kelleher, D., Moore, R., Yurii, K., Byrne, S., Rakovich, Y. P. and Donegan, J. F., "Nonfunctionalized nanocrystals can exploit a cell's active transport machinery delivering them to specific nuclear and cytoplasmic compartments," Nano Lett. 7(11), 3452-3461 (2007).

[29] Sukhanova, A., Susha, A. S., Bek, A., Mayilo, S., Rogach, A. L., Feldmann, J., Oleinikov, V., Reveil, B., Donvito, B. and Cohen, J. H. M., "Nanocrystal-encoded fluorescent microbeads for proteomics: antibody profiling and diagnostics of autoimmune diseases," Nano Lett. 7(8), 2322-2327 (2007).

[30] [http://www.piercenet.com/browse.cfm?fldID=E2C9ED6C-AAC4-4755-AC33-BA209926523B] Pierce Protein Biology Products, Rockford (2011).

[31] Laitinen, O. H., Hytonen, V. P., Nordlund, H. R. and Kulomaa, M. S., "Genetically engineered avidins and streptavidins," Cell. Mol. Life Sci.: CMLS 63(24), 2992-3017 (2006).